MCP Papers in Press. Published on May 5, 2014 as Manuscript M113.036301

The intra viral protein interaction network of hepatitis C virus

Nicole Hagen^{2,*}, Karen Bayer^{1,*}, Kathrin Rösch², Michael Schindler^{1,2,3,#}

¹Institute of Virology, Helmholtz Zentrum Munich, German Research Center for

Environmental Health, Munich, Germany

²Heinrich Pette Institute, Leibniz Institute for Experimental Virology, Hamburg,

Germany

³Institute of Medical Virology and Epidemiology of Viral Diseases, University Clinic

Tübingen, Tübingen, Germany

*These authors contributed equally

#Corresponding author:

Michael Schindler

michael.schindler@helmholtz-muenchen.de

Fon +49-(0)89-3187-4609

Running title: HCV protein interactions

1

Summary

Hepatitis C virus (HCV) is a global health problem and one of the main reasons for chronic liver disease like cirrhosis and hepatocellular carcinoma. The HCV genome is translated into a polyprotein which is proteolytically processed into ten viral proteins. The interactome of the HCV proteins with the host cell has been worked out, however it remains unclear how viral proteins interact with each other. We aimed to generate the interaction network of these ten HCV proteins by a flow cytometry based FRET assay established in our laboratory (Banning et al, 2010 PLoS ONE 5(2): e9344).

HCV proteins were constructed as fusions with the chromophores CFP and YFP. All HCV fusions were expressed and localized to specific subcellular compartments, indicating that they are functional. FACS-FRET measurements identified a total of 20 interactions. 13 of these were previously described and are now confirmed by our method in living cells. Among the seven novel protein binding pairs HCV p7 plays a pivotal role. It binds to the HCV capsid protein Core and the two glycoproteins E1 and E2. These interplays were further demonstrated in the relevant context of Huh7.5 liver cells expressing infectious HCV.

Our work demonstrates the feasibility to rapidly generate small interaction networks by FACS-FRET and defines the network of intra HCV protein interactions. Furthermore, our data supports an important role of p7 in HCV assembly.

Introduction

Hepatitis C virus (HCV) belongs to the family of Flaviviridae and is the only member of the genus Hepacivirus. The ~9.5 kB positive strand RNA genome is directly translated via an internal ribosomal entry site (IRES) into a polyprotein. This is proteolytically processed by cellular and viral proteases into structural (Core, E1, E2) and non-structural (p7, NS2, NS3, NS4A & B and NS5A & B) proteins (1). In the last decades, light was shed on the importance and biological relevance of most HCV proteins which ultimately led to the development of the first specific antiviral therapy by inhibition of the NS3 serine protease (2). However, since HCV is highly variable and there is rapid emergence of drug resistances, additional therapeutic approaches are urgently needed (2). An impressive body of data was derived from protein interaction or siRNA screens investigating the interplay of HCV proteins with cellular factors (3-5). While these screens are essential to understand how HCV manipulates the host cell, their potential benefit for novel therapeutic approaches could be limited. HCV is a chronic viral infection and targeting host factors might result in drugs with severe adverse effects. Thus, a promising strategy would be to specifically inhibit interactions among viral proteins. Surprisingly, until now, a comprehensive analysis of the putative interactions and the interplay of HCV proteins with each other in living human cells is still lacking.

In the present work we did an extensive and thorough analysis of intra HCV protein interactions. We used our novel flow cytometry based FRET assay that allows to

rapidly assess the interplay between proteins in thousands of living cells (6). Therefore this experimental approach enables quantification and statistical evaluation of all results. From the total of 20 interactions established by FACS-FRET we chose to further investigate three which are not yet described in the literature. The putative HCV viroporin p7 binds to the structural proteins and this was verified by biochemical methods in cells expressing fully infectious HCV.

The established network of intra HCV protein interactions in living mammalian cells provides new insights into the biology of this important human pathogen. Furthermore, we identified several HCV protein interactions that could be targeted for antiviral therapy.

Experimental Procedures

Generation of HCV expression plasmids and HCV viral constructs. Each HCV protein was constructed, either as ECFP-fusion, acting as energy donor, or as EYFP-fusion, responding as energy acceptor. All ten HCV proteins were amplified from the HCV JFH1 sequence (7) (Uniprot Q99IB8, molecular clone kindly provided by T. Wakita) and ligated into the pECFP-C1 & pEYFP-C1 vectors (Clontech) via the EcoRI and XhoI restriction sites essentially as described before (6). Mutation RR33/35QQ in p7 was introduced by site directed mutagenesis. Since HCV E1, NS3 and NS5A contain an internal XhoI site, these were cloned into pECFP-N1 & pEYFP-N1 vectors via BsrGI and NotI. HCV-Jc1-E1(A4) and Jc1-E1(A4)-p7(HA) were generated by reconstitution of the H77 strain E1 protein sequence (A4, (8))

SS**GL**Y**H**VTNDC by SOE-PCR within the HCV-Jc1 and Jc1-p7(HA) variants (9), kindly provided by T. Pietschmann. The HCV-Jc1-NS5A(GFP) molecular clone was generously contributed by R. Bartenschlager (10). All PCR derived inserts were sequenced to confirm nucleotide identity.

Cell culture and transfection. 293T and Huh7.5 cells (11) (kindly contributed by C. Rice) were cultivated with Dulbecco's modified Eagle medium (DMEM) supplemented with 10 % fetal calf serum (FCS) plus antibiotics [and 1 % (v/v) nonessential amino-acids for Huh7.5 cells] and grown at 37°C in humidified atmosphere containing 5 % CO₂. 293T single and cotransfections with ECFP and EYFP fusions were performed using the calcium phosphate method. FACS analyses were done 24h post transfection. For this, 150.000 cells/well were seeded in a 12-well plate. In total 2.5μl DNA was transfected, for cotransfection of the fusions an ECFP:EYFP ratio of 1.5:1 was used to compensate the overall lower fluorescence intensity of ECFP and achieve optimal rates of double positive cells. Huh7.5 single and cotransfection with ECFP and EYFP fusions were performed using MetafectenePro (Biontex). FACS analyses were done 48h post transfection. For this, 350.000 cells/well were seeded in a 12-well plate and transfected with 2.0 μl DNA with the protocol provided by the manufacturer.

FACS-based FRET. FACS-FRET was done with a FACS Cantoll Cytometer (BD Bioscience) equipped with 405 nm, 488 nm and 633 nm lasers essentially as described before (6). For EYFP detection, we excited the cells with 488 nm and detected the resulting signal with a 529/24 filter (Semrock). The ECFP signals were

detected via the 450/40 filter (Semrock) after excitation at 405 nm. For FRET cells were exited with 405 nm followed by signal detection with the 529/24 filter again. We used five controls for each cotransfection setup. Mock cells were transfected with water instead of DNA, the vectors pECFP and pEYFP were single-transfected as well as cotransfected to exclude false positive FRET signals and background. An ECFP-EYFP fusion construct was used as positive control. A minimum of 3.000 ECFP and EYFP double positive cells was analysed per measurement.

Electroporation of Huh7.5 cells. After *in vitro* transcription (Promega T7 RiboMAXTM Express Large Scale RNA Production System), HCV_{Jc1} RNA was electroporated (Gene Pulser Xcell System Electroporator; Bio-Rad) into Huh7.5 liver cells essentially as described before (7). In brief, 6.5x10⁶ Huh7.5 cells were washed with PBS, and suspended in 400 μl Cytomix [120 mM KCl, 0.15 mM CaCl₂, 10 mM K₂HPO₄/KH₂PO₄ (pH 7.6), 25 mM Hepes, 2 mM EGTA, 5 mM MgCl₂; pH adjusted to 7.6 with KOH] with freshly added 2 mM ATP and 5 mM glutathione (end-concentration; pH 7.6). After transfer into electroporation cuvettes, 5 μg RNA were pulsed with 975 μF and 270 V. Cells were seeded into well plates or cell tissue flasks (125 cm²). Medium was changed four or sixteen hours after electroporation; cells were analysed 72h later.

Coimmunoprecipitation and Western blot. After lysis of electroporated cells with 800 µl CoIP-lysis buffer [0.05 M Tris, 0.15 M NaCl, 1 mM EDTA, pH 7.4, 1 % TritonX-100] for 20 minutes on a stirring wheel, cell debris was removed by 10 min centrifugation at 14.000 rpm. Supernatants of the lysates were incubated rotating

overnight, together with protease inhibitor (complete mini) and either α -HA(ms) (Sigma) or α -HA(rb) (cell signaling) antibody (1:150). 30 µl protein plus Protein G sepharose were washed three times with CoIP-lysis buffer prior to 4h incubation with antibody-lysate mixture. All steps were performed at 4°C. After washing three times with CoIP-lysis buffer, sepharose was suspended in 20 µl TBS and 15 µl of 5X Laemmli buffer and boiled at 95°C for ten minutes. Samples were analysed via SDS-PAGE and Western blot. After transfer of the separated proteins from the SDS-gel to a nitrocellulosemembrane (0.4 µm; Whatman) and blocking, the membrane was incubated with primary mABs [α -Core (1:1000; C7-50, Abcam), α -E2 (1:1000; AP33, Genentech), α -A4 (1:1000; kindly provided by H. Greenberg and J. Dubuisson) and α -HA(ms) (1:1000)] overnight. Membranes were washed, followed by incubation with the HRP-conjugated secondary antibody (α -mouse, 1:10.000, Sigma) for three hours and washed once again before protein detection.

Confocal microscopy, colocalization analyses and proximity ligation assay. 293T cells or Huh7.5 cells were seeded on coverslips and transfected as described above. Subsequently cells were fixed for 30 min with 2 % PFA and mounted with Mowiol 4-88 (Carl Roth, Karlsruhe) on microscope slides. Confocal microscopy was done with a Zeiss LSM510 with Meta detector or with the Nikon Ti Eclipse equipped with the Perkin Elmer UltraViewVox System (Yokogawa CSU-X1). If not indicated otherwise, we used the HCS NuclearMask Deep Red Stain (Invitrogen) stain for identification of the nuclei. For colocalization studies and PLA Huh7.5 cells were electroporated as described above and seeded on coverslips. 56h post

electroporation cells were fixed for 25 min with 2 % PFA, permeabilized for 15 min with 1 % Saponin and blocked for 45 min with 5 % BSA. Indicated primary antibodies (α -GFP (BioVision), α -NS5A (clone 2F6/G11, IBT), α -CD81 (Ancell), α -HA(rb), α -core, α -E2, α -A4) were incubated 1:100 in 1 % BSA for 2 h at RT. For colocalization studies AlexaFluor 405, 488 or 555 anti-mouse or –rabbit were incubated for 1 h respectively and mounted with Mowiol 4-88. For PLA secondary antibody probes, ligation reaction and amplification were assessed according to the protocol of the manufacturer (Duolink, Sigma Aldrich). Spinning disc microscopy was done with the Nikon Ti Eclipse UltraViewVox System. Image analysis was done with the Volocity 6.2 software package. For colocalization every cell was cropped and Pearson's R² value calculated accordingly to Costes colocalization. For PLA software implemented automated spot counting was used.

Generation of the interaction network. The interaction map was constructed with the open source program Cytoscape (www.cytoscape.org). Intra-viral HCV protein-interactions found within the present study by FACS-FRET and published previously (compare Fig. 3) were summarized in one map (Fig. 9). Additionally, we incorporated the interaction of HCV proteins with the host cell. For this, interaction data of the VirusMint database (mint.bio.uniroma2.it) and from de Chassey et al. (4) – who did a proteome-wide interaction screen for HCV – were included. The VirusMint dataset was cleared of double and reverse tested interactions and those which were exclusively defined by colocalization studies.

Statistical analyses. Statistical analyses were performed with the Graph Pad Prism software version 5.0. We used the two-tailed unpaired Student's t test to statistically assess differences between FRET and background signals (respective CFP-fusion protein cotransfected with YFP-only). Pearson values were calculated for correlation analyses. For the colocalization and PLA results we used the one-way ANOVA with Bonferroni post-test to assess significance levels.

Results

Characterization of fluorescently tagged HCV fusion proteins.

In order to define the network of intra HCV protein interactions by FACS-FRET we fused all ten viral proteins of the JFH1 strain (7) with the chromophores CFP and YFP. Since a chromophore tag can alter the stability of a protein, we first checked proper expression by Western blot. Linkage of CFP or YFP to the C-terminus of the HCV Core, E1 and E2 completely abrogated protein expression although we introduced a methionine start codon at the beginning of each ORF (data not shown). In contrast, all HCV proteins were expressed when we fused the chromophores at the N-terminus, albeit with different efficiencies (Fig. 1A). Additionally, we measured expression of the various HCV fusion proteins by FACS parameters, i.e. the fluorescence intensity relative to YFP or CFP and the total percentage of transfected cells (Fig. 1B). These parameters correlated significantly for the YFP and CFP HCV fusions (Fig. 1C) and allowed us to detect also proteins that showed very weak

expression by Western blot (e.g. YFP-NS4A; note that CFP-NS4A could not be detected by WB).

Chromophore tags are generally well tolerated (12). Nevertheless they can affect the localization of a protein and thus its functionality. We therefore investigated the subcellular distribution of the YFP/CFP fused HCV proteins by confocal microscopy. HCV proteins are associated with intracellular membranes (e.g. the ER) and lipids. In line with this, all YFP/CFP HCV fusion proteins showed an ER-like or punctuated subcellular distribution (Fig. 1D). In contrast, none of the fusions was diffusely expressed within the cell nor did they localize to the nucleus.

Altogether, we conclude that the generated YFP/CFP HCV fusion proteins are useful tools to assess the network of intra HCV protein interactions by FACS-FRET.

Analysis of specific HCV protein interactions by FACS-FRET.

As proof-of-principle we next aimed to validate a set of previously described interactions with our method. In Figure 2 we present confocal images of the subcellular localization of the fusion proteins (panel 1) and representative FACS-plots (panel 2) as well as a summary generated from multiple independent biological replicates including statistics (panel 3). For FACS-FRET we first gated on double positive cells expressing both YFP and CFP and then plotted the CFP intensity versus FRET (see Fig.2, Panel 2). Gates are generated according to the negative (cotransfection of YFP and CFP) and the positive control (transfection of a YFP-CFP fusionprotein), which generally resulted in less than 0.5 % of FRET+ cells for the

negative control and more than 95 % of FRET+ cells for the positive control (6). We furthermore analysed at least 3.000 double positive cells per transfection.

When we assessed heterodimer formation of the HCV glycoproteins E1 and E2 (8, 13) (Fig. 2A), we measured 74.8 % FRET+ cells (SD±17.68 %; n=17) in 293T cells and confirmed this result in the liver cell line Huh7.5 (MF=42.2 %; SD±10.45; n=7). Furthermore we confirmed multimerization of the HCV Core protein (14, 15) which is essential for nucleocapsid formation (Fig. 2B; MF=67.9 %; SD±14.88; n=9 in 293T cells and MF=44.9 %; SD±25.25; n=8 in Huh7.5). In contrast, we failed to verify the interaction of E2 with the NS3 protease (16) in our system (Fig. 2C; MF<10 % in both cell lines). Of note, in contrast to E1 and E2 heterodimer formation and Core multimerization, we also failed to detect areas of pronounced colocalization when we assessed the subcellular distribution of E2 and NS3 (Fig. 2). This is in-line with the absence of robust FRET measured by flow cytometry.

Thus, our measurements reveal some differences to previous observations. Nevertheless, we could verify important and well established interactions in living 293T and Huh7.5 liver cells by our FACS-FRET approach.

HCV protein interactions determined by FACS-FRET.

To establish the complete network of intra HCV protein interactions we tested all fusion proteins in two combinations: YFP-protein A with CFP-protein B and vice versa YFP-protein B with CFP-protein A. Extensive FACS-FRET measurements and colocalization analyses were performed after cotransfection of both constructs in

293T cells (see supplemental data set). The FRET signal of the negative control – i.e. YFP-only cotransfected with CFP-only – generally resulted in a signal of less than 2 % FRET+ cells (average value 0.49 %; SD±0.93; n=190).

The quantitative results of all measurements are summarized in the supplemental Figure S1 and the qualitative overview is presented in Figure 3. For each of the 100 possible combinations we indicated the following parameters: n, number of biological replicates; MF, mean value % FRET+ cells; SD, standard deviation; significance value. We used the two-tailed unpaired Student's t test to statistically challenge observed differences between FRET and background signals. Background is defined by an additional negative control i.e. the respective CFP-fusion protein cotransfected with YFP-only for each experiment. We furthermore arbitrarily introduced an additional stringency threshold of 10 % FRET+ cells for interactions (Fig. S1 values in red). Therefore, some FRET signals below the threshold can be significantly higher than the background but are considered as not relevant (Fig. S1 values in green). 293T cells are kidney derived and were used for FACS-FRET since they are an established and easy to transfect mammalian cell system that allows overexpression of proteins (6). However, hepatitis C virus has a strong liver cell tropism (12). Thus, interactions of viral proteins could be different in the presence of liver cell specific factors. We therefore assessed a total of 45 interactions by FACS-FRET in Huh7.5 liver cells (11). These analyses included all those that were over the 10 % threshold in 293T cells. The background signal of the negative control for Huh7.5 transfections was 0.29 % FRET+ cells (±0.97; n=82). The results were analysed similar to the data

obtained from 293T cells and incorporated in Figure S1. Although the absolute percentage of FRET+ cells varied between both cell types, interactions found in 293T cells could generally be confirmed in Huh7.5 cells. Hence the results obtained from both cell lines correlated significantly (see inlay Fig. 3; R²=0.6317; p<0.0001; n=45). Altogether, as depicted in the consolidated summary Figure 3, we report by FACS-FRET a total of twenty interactions in living mammalian cells (p<0.05 and MF≥10 %). Eleven could be detected in both cell lines (Core/Core, E1/E2, E1/NS5B, E2/E2, E2/p7, E2/NS2, E2/NS5B, p7/NS2, NS2/NS2, NS3/NS3, NS5A/NS5A) whereas the other nine interactions reached our criteria only in 293T cells (Core/E2, Core/p7, Core/NS2, Core/NS5B, E1/p7, E1/NS2, p7/p7, NS3/NS4A, NS4B/NS4B). Most importantly, seven of the twenty protein interactions determined by FACS-FRET have not been described in the literature before (Fig. 3 and Fig. 4). Binding of E2/p7, NS5B/E1 and NS5B/E2 were observed in both cell lines (Fig. 4A). In contrast, FRET signals between E2/Core, NS2/Core, p7/Core and p7/E1 were only significant and above the 10 % threshold in 293T cells (Fig. 4B).

In sum, we established the intra HCV interactome by FACS-FRET. Thereby we succeeded to confirm a variety of interactions in the context of living mammalian cells. Moreover, our novel approach revealed a set of previously unrecognized HCV protein interactions that might be important during viral replication.

Residues RR33/35 in p7 mediate interaction with E2.

It has been reported that p7 is important for HCV production and mutation of a dibasic motif RR33/35QQ in HCV-JFH1 p7 disrupts virus production without a defect at the level of E2-p7-NS2 processing (17). However, the molecular determinants for the defect of the p7-RR/QQ mutant are still elusive and we hypothesized that the mutation might affect intra viral p7 protein interactions. We thus changed the arginines at position 33 and 35 in JFH1 p7-CFP/YFP to glutamine. Next, we investigated the multimerization of the p7-RR/QQ mutant and wt JFH-1 p7 as well as their interaction with Core, E1 and E2 by FACS-FRET (Fig. 5). Changing the dibasic R motif to Q slightly – albeit significantly – affected the interaction of p7 with Core and E1 as well as oligomerization (see primary FACS plots in Fig. 5A and the quantitative analyses of multiple replicates in Fig. 5B). In contrast, mutation of p7 RR33/35QQ strongly disrupts p7 interaction with E2 (Fig. 5).

We conclude that the dibasic arginine motif at positions 33 and 35 in JFH1 p7 might be involved in interaction with E2. Moreover, this data demonstrates that our system can contribute to elucidate molecular determinants of virological phenotypes.

Detection of p7 binding to Core, E1 and E2 by coimmunoprecipitation.

For FACS-FRET viral proteins were fused with chromophores and overexpressed in 293T or Huh7.5 liver cells. Previously we could confirm in a variety of studies that positive FACS-FRET results can be verified by biochemical methods and with untagged proteins (6, 18-20). Nevertheless, in the context of a dynamic viral infection

expression levels might substantially vary and other viral proteins might affect specific interactions.

We aimed to verify interactions discovered by FACS-FRET in HCV expressing Huh7.5 cells. As far as we know, no specific antibodies are available for detection of either E1 or p7 from JFH1 or Jc1. However, it is possible to stain the E1-A4 epitope derived from HCV-H77 by immunoblot (8). Hence, we reconstituted the E1-A4 sequence in the HCV-Jc1 backbone and the HCV-Jc1 HA-p7 construct (9) in order to be able to analyse E1 and p7 with biochemical techniques.

To achieve high expression levels Huh7.5 cells were electroporated with *in vitro* transcribed RNA of the respective construct. Quantification of electroporation efficiency by intracellular FACS-staining confirmed that generally more than 40 % of cells were HCV positive (not shown). Coimmunoprecipitation with an anti-HA-antibody from rabbit revealed specific interaction of p7 with E2 and E1 (Fig. 6, upper bands). Unfortunately, the migration pattern of the light chain of this antibody did not allow detection of Core at ~21 kD. Thus, we repeated the IP with a mouse derived anti-HA-antibody and could now detect specific interaction of HA-p7 with Core (Fig. 6, lower band). These results demonstrate that p7 interacts with the HCV structural proteins in liver cells expressing fully infectious HCV.

The HCV structural proteins interact with p7 in virus expressing intact Huh7.5 liver cells.

FRET allows detecting transient dynamic interactions in the physiological environment of the cell (6, 12). Since two putative interaction partners need to be in close proximity for robust FRET – usually less than 10 nm – there has to be a substantial degree of colocalization between two binding partners. We thus investigated the colocalization of HCV proteins in virus expressing Huh7.5 cells.

As positive control we electroporated Huh7.5 cells with the HCV Jc1-NS5A(GFP) construct expressing an NS5A-GFP fusion protein (10). Then we did immunofluorescence staining with NS5A and GFP specific antibodies, necessarily reflecting a high degree of colocalization quantified by the squared Pearson's colocalization coefficient (R²=0.676, Fig. 7A and mean R²=0.5581 ±0.0479 SEM, Fig. 7B). In contrast, we were surprised to see some colocalization between NS5A-GFP and CD81, although R² values were significantly lower (see Fig. 7A and B).

Next we used the Jc1-E1(A4)-p7(HA) variant to quantify colocalization between p7 by HA-staining and the HCV structural proteins. There was a complete absence of colocalization between p7(HA) and CD81 (mean R^2 =0.1804 ±0.0264 SEM). In contrast Core, E2 and E1(A4) colocalized with p7(HA) and the mean R^2 values were significantly higher than those measured for p7(HA) and CD81 (see Figure 7A and B, mean R^2 values were 0.3859 for p7(HA)/Core, 0.5731 for p7(HA)/E2 and 0.5476 for p7(HA)/E1(A4), respectively). Thus, the viral structural proteins colocalize with p7 in HCV expressing Huh7.5 cells.

Colocalization indicates the presence of two putative binding partners in the same subcellular region and is a hint but not a proof for direct interaction. We therefore

decided to exploit proximity ligation assay (PLA) (21) to demonstrate direct interactions of the viral proteins in intact cells. PLA can be done with the same primary antibodies that were used for immunofluorescence. When these are in close proximity the secondary PLA antibodies trigger an enzymatic reaction followed by a rolling circle amplification of fluorescent oligonucleotide probes. Thus, when two proteins interact within a cell, a bright fluorescent spot visualizes this event. We first did control stainings in Huh7.5 cells with the single primary antibodies and the PLA probes to exclude unspecific binding, which did not result in detectable PLA spots (data not shown). We then repeated the setting of the colocalization experiment presented in Figure 7, but used PLA probes as secondary antibodies. As a read out we counted the amount of PLA spots per cell and analysed a minimum of ten cells per staining (Fig. 8). The positive control, which is detection of the NS5A-GFP fusion by specific NS5A and GFP antibodies, resulted in an average number of 78 spots/cell whereas NS5A-GFP showed no PLA signal with CD81 (Fig. 8A and B). Thus, despite a certain degree of colocalization between NS5A-GFP and CD81 (compare Fig. 7) the negative PLA result argues against a direct interaction of these two proteins. In contrast, all structural HCV proteins gave high PLA signals with p7(HA) which were in the range of the positive control (see Figure 8A and B, mean number of PLA spots/cell 55 for p7(HA)/Core, 61 for p7(HA)/E2 and 67 for p7(HA)/E1(A4)). Importantly, the negative control, which was PLA measured between p7(HA) and CD81 gave only background signals (3 spots/cell) and calculated differences were highly significant (Fig. 8B).

Altogether, the cumulated data of the colocalization and PLA experiments strongly suggest that HCV p7 interacts with the viral structural proteins Core, E1 and E2 in intact and HCV expressing Huh7.5 liver cells.

Discussion

We performed a comprehensive assessment of intra HCV protein interactions with a FACS-based FRET assay in intact cells. This analysis revealed a set of 20 protein-protein interactions that met our stringency threshold and thus exerted robust FRET. By thorough literature mining we found that 13 interactions were previously described with alternative techniques (compare Fig. 3). Therefore, we confirm for the first time their association in living cells. In addition, the seven protein interaction pairs newly discovered by us comprise mainly the structural proteins. HCV p7 binds to Core, E1 and E2 and interaction of p7 with E2 seems important for virus production. Furthermore Core was found to exert FRET with E2 and NS2 and this whole complex might have a pivotal role for HCV assembly and egress. In addition we report significant FRET for NS5B together with E1 and E2. From a biological point of view, the possible importance of the latter interactions remains elusive.

FACS-FRET has a variety of striking advantages that render this technique superior to other methods to detect protein interactions (6, 22). Nevertheless, one serious constraint is the necessity to use fusion proteins with chromophores. These tags can impair functionality and expression of the native proteins. We extensively tested expression levels by FACS and WB and checked the subcellular localization of the transfected fusions. HCV Core, E1 and E2 with a C-terminal chromophore tag were

not expressed at all and as expected, expression levels of the N-terminal fusions varied (see Figure 1 for details). However, the specific localization to distinct subcellular compartments indicated that the HCV fusion proteins are properly expressed, although we cannot exclude impairments in functionality. At least for the non-structural proteins a large body of published data working with tagged HCV fusion proteins, employing HIS, FLAG, HA, GST and GFP tags supports no major functional impairments as a consequence of the tag (9, 10, 16, 23-29).

In contrast to the various *in situ* and precipitation techniques FRET works in living and intact cells, supporting interactions in physiological conditions of the cellular environment. Furthermore, proteins bind each other in their natural subcellular compartment, which is a clear advantage in comparison to yeast-two-hybrid systems (6). Nevertheless cellular proteins are important determinants for HCV replication and we have to consider the possibility, that liver cell specific factors also influence intra viral protein interactions (3, 5). We thus conducted experiments in 293T and Huh7.5 cells revealing in general a significant correlation between the results in both cell types. In line with this, it was recently demonstrated that the exogenous expression of HCV entry receptors, the microRNA miR122 and ApolipoproteinE is sufficient to achieve completion of the whole HCV life cycle in 293T cells (30). We therefore postulate that major differences in FRET, which we observed occasionally between 293T and Huh7.5 cells (compare Fig. 4B), are most likely attributable to the lower levels of protein expression in the liver cell line.

Another problem we encountered are major differences in the percentages of FRET+ cells depending on the usage of CFP and YFP as either donor or acceptor. One extreme example is the well-established interaction between the glycoproteins E1 and E2 (8, 13, 31). Assessing FRET between CFP-E2 and YFP-E1 results in 74.8 % FRET+ cells whereas transfection of CFP-E1 together with YFP-E2 did not give any FRET at all (Figs. 2 and S1). This phenomenon has been described before and can be explained by the donor:acceptor stoichiometry (32, 33). FRET is generally more efficient when there is an excess of acceptor molecules. Therefore a ratio of 1:2 gives higher FRET than 2:1 (32). In addition, Koushik and colleagues performed elegant experiments demonstrating continuously higher FRET correlating with increasing amounts of acceptor (33). Thus, we generally tested both possible donor acceptor combinations to eliminate potential loss of FRET as a reason of different donor:acceptor quantities.

Apart from the restrictions addressed and discussed above we postulate that FACS-based FRET is currently one of the gold standard techniques to investigate protein interactions. We established and used this technique in the past to demonstrate and map for instance the interaction of HIV-1 Vpu and Ebola GP2 with the antiviral factor Tetherin/Bst-2 (6, 18, 19) and to show the interplay between HIV-1 Gag and tetraspanins (34). Also other groups used our FACS-FRET approach to show direct protein interactions confirming independently the robustness of the assay (35-38). Of note, Kim and coworkers systematically compared FACS-FRET, BRET (bioluminescence resonance energy transfer) and FLIM (fluorescence lifetime

imaging microscopy) (22). In this study, the same potential interaction partners of the amyloid precursor protein (APP) were studied using all the three different methods. They concluded that FACS-FRET is the most sensitive and reliable approach to investigate protein interactions with a superior Z-score as indicator for high throughput screening compatibility.

Nevertheless we analysed the results from our FACS-FRET approach with high stringency. Experiments were performed in two cell lines and an extensive number of biological replicates were conducted by different individuals. Subsequently, statistics were used to assess the significance of identified interactions versus the negative control. Furthermore, an additional stringency threshold of 10 % was introduced. Only percentages of FRET+ cells higher than 10 % were considered as 'true'. Thus, the interactions discussed and presented have a high statistical confidence. The reliability of the whole screening approach is also reflected by the fact that we confirmed three of the seven newly found interactions by alternative techniques. Strikingly, interaction of p7 with Core, E1 and E2 could be demonstrated by coimmunoprecipitation, immunofluorescence and the proximity ligation assay (PLA) in Huh7.5 liver cells expressing replicating and fully infectious hepatitis C virus. Apart from that, E1 and E2 showed significant FRET with NS5B in 293T and Huh7.5 cells (Fig. 4A). Indeed, interaction of NS5B with the two glycoproteins and Core, which we also found by FACS-FRET could participate in correct coordination of assembly and RNA genome incorporation. However, this hypothesis has to be experimentally

followed up in further experiments, although a recent study suggests a role of NS5B in HCV assembly (39).

It is remarkable that most of the interactions reported herein refer to structural proteins and NS2 and p7 (Figure 3 and 9). In contrast, we detected nearly no FRET between the non-structural (NS) proteins as well as the NS and structural proteins. The discrepancy to published NS interactions could be explained by the techniques used. In contrast to previously exploited coIP, FRET cannot detect higher molecular complexes due to the increasing Foerster's radius (12, 40). Thus it is tempting to speculate that the HCV NS proteins form higher molecular complexes among themselves and with the structural proteins, whereas the structural proteins directly interact with each other. This further emphasizes that the newly described interactions herein might be critically involved in HCV assembly. In this context direct binding of p7 and Core was postulated before (41) and a variety of hints for interaction of these proteins are published in the literature (42-44). For instance, Popescu and colleagues reported that Core, the envelope proteins, and p7 influence subcellular NS2 localization (23). Using FACS-FRET, coIP and PLA we could demonstrate for the first time that there is a direct interaction between p7 and Core as well as between NS2 and Core. These findings could give a functional rational for previously published data. Furthermore, it was suggested that E2 and p7 might interact (9, 44, 45) and Gentzsch and colleagues postulated that the p7-RR/QQ mutant has a defect at the step of capsid envelopment. Strikingly, our data suggests that mutation of the dibasic motif in p7 selectively impairs the interaction with E2 (44).

Thus, our FACS-FRET analyses provides a mechanistic explanation for the virological phenotype of this mutant.

Incorporating interaction data from the VirusMINT database [http://mint.bio.uniroma2.it/virusmint] and the work by de Chassey and colleagues (4) into our intra HCV protein interaction network suggests the existence of three major nodes HCV uses to manipulate the host cell (Fig. 9). As already pointed out, most proteins might indirectly interact by higher molecular complexes. However, the direct interaction network of Core, E1, E2, p7, NS2 and NS5B is connected to the host cell mainly by the multiple virus-host interactions exerted by Core. Two other clusters comprise the NS3:NS4 protease with NS3 as main communicator with host factors and the HCV NS5A, which is an important cofactor for HCV replication (46, 47). Thus, the single viral proteins Core, NS3 and NS5A within the direct interaction clusters could serve as interfaces for HCV mediated manipulation of the host cell. In sum, we postulate that the newly described interactions herein contribute to the formation of an HCV assembly network. In addition our data underline and support the pivotal role of p7 in HCV morphogenesis (9, 17, 41-44, 48, 49). In the future it will be of high interest to use FACS-FRET in order to map interaction domains important for the diverse intra HCV protein interactions and to correlate mutations in viral proteins with virological parameters, as demonstrated here for the p7-RR/QQ mutant. Similar experiments could be done for patient derived and thus evolutionary shaped viral proteins. Such approaches will shed light on the biological relevance of the diverse intra HCV protein interactions and are highly warranted.

Acknowledgements

The authors thank Ulrike Protzer for constant support and encouragement, Ruth Brack-Werner for helpful discussions and Eike Steinmann and Eva Herker for critical reading of the manuscript. In addition, we are very grateful to Thomas Pietschmann, Ralf Bartenschlager, Charles Rice, Takaji Wakita, Harry Greenberg and Jean Dubuisson for the generous contribution of reagents. Nicole Hagen was supported by a scholarship of the SDI (Structure and Dynamics in Infection) graduate school Hamburg and a stipend from the Pro Exzellenzia (Hamburger Hochschulen für Frauen). This work was supported by institutional funding received from the Heinrich Pette Institute, Leibniz Institute for Experimental Virology, Hamburg and the Helmholtz Zentrum Munich, German Research Center for Environmental Health.

References

- 1. Moradpour, D., Penin, F., and Rice, C. M. (2007) Replication of hepatitis C virus. *Nature reviews*. *Microbiology* 5, 453-463
- 2. Kronenberger, B., and Zeuzem, S. (2012) New developments in HCV therapy. *Journal of viral hepatitis* 19 Suppl 1, 48-51
- 3. Tai, A. W., Benita, Y., Peng, L. F., Kim, S. S., Sakamoto, N., Xavier, R. J., and Chung, R. T. (2009) A functional genomic screen identifies cellular cofactors of hepatitis C virus replication. *Cell host & microbe* 5, 298-307
- 4. de Chassey, B., Navratil, V., Tafforeau, L., Hiet, M. S., Aublin-Gex, A., Agaugue, S., Meiffren, G., Pradezynski, F., Faria, B. F., Chantier, T., Le Breton, M., Pellet, J., Davoust, N., Mangeot, P. E., Chaboud, A., Penin, F., Jacob, Y., Vidalain, P. O., Vidal, M., Andre, P., Rabourdin-Combe, C., and Lotteau, V. (2008) Hepatitis C virus infection protein network. *Molecular systems biology* 4, 230
- 5. Li, Q., Brass, A. L., Ng, A., Hu, Z., Xavier, R. J., Liang, T. J., and Elledge, S. J. (2009) A genome-wide genetic screen for host factors required for hepatitis C virus propagation. *Proceedings of the National Academy of Sciences of the United States of America* 106, 16410-16415

- 6. Banning, C., Votteler, J., Hoffmann, D., Koppensteiner, H., Warmer, M., Reimer, R., Kirchhoff, F., Schubert, U., Hauber, J., and Schindler, M. (2010) A flow cytometry-based FRET assay to identify and analyse protein-protein interactions in living cells. *PloS one* 5, e9344
- 7. Wakita, T., Pietschmann, T., Kato, T., Date, T., Miyamoto, M., Zhao, Z., Murthy, K., Habermann, A., Krausslich, H. G., Mizokami, M., Bartenschlager, R., and Liang, T. J. (2005) Production of infectious hepatitis C virus in tissue culture from a cloned viral genome. *Nature medicine* 11, 791-796
- 8. Dubuisson, J., Hsu, H. H., Cheung, R. C., Greenberg, H. B., Russell, D. G., and Rice, C. M. (1994) Formation and intracellular localization of hepatitis C virus envelope glycoprotein complexes expressed by recombinant vaccinia and Sindbis viruses. *Journal of virology* 68, 6147-6160
- 9. Vieyres, G., Brohm, C., Friesland, M., Gentzsch, J., Wolk, B., Roingeard, P., Steinmann, E., and Pietschmann, T. (2013) Subcellular localization and function of an epitope-tagged p7 viroporin in hepatitis C virus-producing cells. *Journal of virology* 87, 1664-1678
- 10. Schaller, T., Appel, N., Koutsoudakis, G., Kallis, S., Lohmann, V., Pietschmann, T., and Bartenschlager, R. (2007) Analysis of hepatitis C virus superinfection exclusion by using novel fluorochrome gene-tagged viral genomes. *Journal of virology* 81, 4591-4603
- 11. Blight, K. J., McKeating, J. A., and Rice, C. M. (2002) Highly permissive cell lines for subgenomic and genomic hepatitis C virus RNA replication. *Journal of virology* 76, 13001-13014
- 12. Siegel, R. M., Chan, F. K., Zacharias, D. A., Swofford, R., Holmes, K. L., Tsien, R. Y., and Lenardo, M. J. (2000) Measurement of molecular interactions in living cells by fluorescence resonance energy transfer between variants of the green fluorescent protein. *Science's STKE : signal transduction knowledge environment* 2000, pl1
- 13. Ralston, R., Thudium, K., Berger, K., Kuo, C., Gervase, B., Hall, J., Selby, M., Kuo, G., Houghton, M., and Choo, Q. L. (1993) Characterization of hepatitis C virus envelope glycoprotein complexes expressed by recombinant vaccinia viruses. *Journal of virology* 67, 6753-6761
- 14. Matsumoto, M., Hwang, S. B., Jeng, K. S., Zhu, N., and Lai, M. M. (1996) Homotypic interaction and multimerization of hepatitis C virus core protein. *Virology* 218, 43-51
- 15. Mousseau, G., Kota, S., Takahashi, V., Frick, D. N., and Strosberg, A. D. (2011) Dimerization-driven interaction of hepatitis C virus core protein with NS3 helicase. *The Journal of general virology* 92, 101-111
- 16. Flajolet, M., Rotondo, G., Daviet, L., Bergametti, F., Inchauspe, G., Tiollais, P., Transy, C., and Legrain, P. (2000) A genomic approach of the hepatitis C virus generates a protein interaction map. *Gene* 242, 369-379
- 17. Steinmann, E., Penin, F., Kallis, S., Patel, A. H., Bartenschlager, R., and Pietschmann, T. (2007) Hepatitis C virus p7 protein is crucial for assembly and release of infectious virions. *PLoS pathogens* 3, e103
- 18. Bolduan, S., Votteler, J., Lodermeyer, V., Greiner, T., Koppensteiner, H., Schindler, M., Thiel, G., and Schubert, U. (2011) Ion channel activity of HIV-1 Vpu is dispensable for counteraction of CD317. *Virology* 416, 75-85
- 19. Kuhl, A., Banning, C., Marzi, A., Votteler, J., Steffen, I., Bertram, S., Glowacka, I., Konrad, A., Sturzl, M., Guo, J. T., Schubert, U., Feldmann, H., Behrens, G., Schindler, M., and Pohlmann, S. (2011) The Ebola virus glycoprotein and HIV-1 Vpu employ different strategies to counteract the antiviral factor tetherin. *The Journal of infectious diseases* 204 Suppl 3, S850-860
- 20. Hoffmann, D., Schwarck, D., Banning, C., Brenner, M., Mariyanna, L., Krepstakies, M., Schindler, M., Millar, D. P., and Hauber, J. (2012) Formation of trans-activation competent HIV-1

- Rev:RRE complexes requires the recruitment of multiple protein activation domains. *PloS one* 7, e38305
- 21. Fredriksson, S., Gullberg, M., Jarvius, J., Olsson, C., Pietras, K., Gustafsdottir, S. M., Ostman, A., and Landegren, U. (2002) Protein detection using proximity-dependent DNA ligation assays. *Nature biotechnology* 20, 473-477
- 22. Kim, J., Lee, J., Kwon, D., Lee, H., and Grailhe, R. (2011) A comparative analysis of resonance energy transfer methods for Alzheimer related protein-protein interactions in living cells. *Molecular bioSystems* 7, 2991-2996
- 23. Popescu, C. I., Callens, N., Trinel, D., Roingeard, P., Moradpour, D., Descamps, V., Duverlie, G., Penin, F., Heliot, L., Rouille, Y., and Dubuisson, J. (2011) NS2 protein of hepatitis C virus interacts with structural and non-structural proteins towards virus assembly. *PLoS pathogens* 7, e1001278
- 24. Frick, D. N., Rypma, R. S., Lam, A. M., and Gu, B. (2004) The nonstructural protein 3 protease/helicase requires an intact protease domain to unwind duplex RNA efficiently. *The Journal of biological chemistry* 279, 1269-1280
- 25. Ma, Y., Anantpadma, M., Timpe, J. M., Shanmugam, S., Singh, S. M., Lemon, S. M., and Yi, M. (2011) Hepatitis C virus NS2 protein serves as a scaffold for virus assembly by interacting with both structural and nonstructural proteins. *Journal of virology* 85, 86-97
- 26. Dimitrova, M., Imbert, I., Kieny, M. P., and Schuster, C. (2003) Protein-protein interactions between hepatitis C virus nonstructural proteins. *Journal of virology* 77, 5401-5414
- 27. Cho, H. S., Ha, N. C., Kang, L. W., Chung, K. M., Back, S. H., Jang, S. K., and Oh, B. H. (1998) Crystal structure of RNA helicase from genotype 1b hepatitis C virus. A feasible mechanism of unwinding duplex RNA. *The Journal of biological chemistry* 273, 15045-15052
- 28. Shimakami, T., Hijikata, M., Luo, H., Ma, Y. Y., Kaneko, S., Shimotohno, K., and Murakami, S. (2004) Effect of interaction between hepatitis C virus NS5A and NS5B on hepatitis C virus RNA replication with the hepatitis C virus replicon. *Journal of virology* 78, 2738-2748
- 29. Wolk, B., Buchele, B., Moradpour, D., and Rice, C. M. (2008) A dynamic view of hepatitis C virus replication complexes. *Journal of virology* 82, 10519-10531
- 30. Da Costa, D., Turek, M., Felmlee, D. J., Girardi, E., Pfeffer, S., Long, G., Bartenschlager, R., Zeisel, M. B., and Baumert, T. F. (2012) Reconstitution of the entire hepatitis C virus life cycle in nonhepatic cells. *Journal of virology* 86, 11919-11925
- 31. Yi, M., Nakamoto, Y., Kaneko, S., Yamashita, T., and Murakami, S. (1997) Delineation of regions important for heteromeric association of hepatitis C virus E1 and E2. *Virology* 231, 119-129
- 32. Chen, H., Puhl, H. L., 3rd, Koushik, S. V., Vogel, S. S., and Ikeda, S. R. (2006) Measurement of FRET efficiency and ratio of donor to acceptor concentration in living cells. *Biophysical journal* 91, L39-41
- 33. Koushik, S. V., Blank, P. S., and Vogel, S. S. (2009) Anomalous surplus energy transfer observed with multiple FRET acceptors. *PloS one* 4, e8031
- 34. Koppensteiner, H., Banning, C., Schneider, C., Hohenberg, H., and Schindler, M. (2012) Macrophage internal HIV-1 is protected from neutralizing antibodies. *Journal of virology* 86, 2826-2836
- 35. Thyrock, A., Stehling, M., Waschbusch, D., and Barnekow, A. (2010) Characterizing the interaction between the Rab6 GTPase and Mint3 via flow cytometry based FRET analysis. *Biochemical and biophysical research communications* 396, 679-683

- 36. Somvanshi, R. K., Chaudhari, N., Qiu, X., and Kumar, U. (2011) Heterodimerization of beta2 adrenergic receptor and somatostatin receptor 5: Implications in modulation of signaling pathway. *Journal of molecular signaling* 6, 9
- 37. Asbach, B., Ludwig, C., Saksela, K., and Wagner, R. (2012) Comprehensive analysis of interactions between the Src-associated protein in mitosis of 68 kDa and the human Src-homology 3 proteome. *PloS one* 7, e38540
- 38. Hassinen, A., Pujol, F. M., Kokkonen, N., Pieters, C., Kihlstrom, M., Korhonen, K., and Kellokumpu, S. (2011) Functional organization of Golgi N- and O-glycosylation pathways involves pH-dependent complex formation that is impaired in cancer cells. *The Journal of biological chemistry* 286, 38329-38340
- 39. Gouklani, H., Bull, R. A., Beyer, C., Coulibaly, F., Gowans, E. J., Drummer, H. E., Netter, H. J., White, P. A., and Haqshenas, G. (2012) Hepatitis C virus nonstructural protein 5B is involved in virus morphogenesis. *Journal of virology* 86, 5080-5088
- 40. Piston, D. W., and Kremers, G. J. (2007) Fluorescent protein FRET: the good, the bad and the ugly. *Trends in biochemical sciences* 32, 407-414
- 41. Boson, B., Granio, O., Bartenschlager, R., and Cosset, F. L. (2011) A concerted action of hepatitis C virus p7 and nonstructural protein 2 regulates core localization at the endoplasmic reticulum and virus assembly. *PLoS pathogens* 7, e1002144
- 42. Gouklani, H., Beyer, C., Drummer, H., Gowans, E. J., Netter, H. J., and Haqshenas, G. (2013) Identification of specific regions in hepatitis C virus core, NS2 and NS5A that genetically interact with p7 and coordinate infectious virus production. *Journal of viral hepatitis* 20, e66-71
- 43. Bentham, M. J., Foster, T. L., McCormick, C., and Griffin, S. (2013) Mutations in hepatitis C virus p7 reduce both the egress and infectivity of assembled particles via impaired proton channel function. *The Journal of general virology* 94, 2236-2248
- 44. Gentzsch, J., Brohm, C., Steinmann, E., Friesland, M., Menzel, N., Vieyres, G., Perin, P. M., Frentzen, A., Kaderali, L., and Pietschmann, T. (2013) hepatitis c Virus p7 is critical for capsid assembly and envelopment. *PLoS pathogens* 9, e1003355
- 45. Atoom, A. M., Jones, D. M., and Russell, R. S. (2013) Evidence suggesting that HCV p7 protects E2 glycoprotein from premature degradation during virus production. *Virus research* 176, 199-210
- 46. Tellinghuisen, T. L., Foss, K. L., and Treadaway, J. (2008) Regulation of hepatitis C virion production via phosphorylation of the NS5A protein. *PLoS pathogens* 4, e1000032
- 47. Huang, L., Hwang, J., Sharma, S. D., Hargittai, M. R., Chen, Y., Arnold, J. J., Raney, K. D., and Cameron, C. E. (2005) Hepatitis C virus nonstructural protein 5A (NS5A) is an RNA-binding protein. *The Journal of biological chemistry* 280, 36417-36428
- 48. Wozniak, A. L., Griffin, S., Rowlands, D., Harris, M., Yi, M., Lemon, S. M., and Weinman, S. A. (2010) Intracellular proton conductance of the hepatitis C virus p7 protein and its contribution to infectious virus production. *PLoS pathogens* 6, e1001087
- 49. Brohm, C., Steinmann, E., Friesland, M., Lorenz, I. C., Patel, A., Penin, F., Bartenschlager, R., and Pietschmann, T. (2009) Characterization of determinants important for hepatitis C virus p7 function in morphogenesis by using trans-complementation. *Journal of virology* 83, 11682-11693
- 50. Serebrov, V., and Pyle, A. M. (2004) Periodic cycles of RNA unwinding and pausing by hepatitis C virus NS3 helicase. *Nature* 430, 476-480

- 51. Locatelli, G. A., Spadari, S., and Maga, G. (2002) Hepatitis C virus NS3 ATPase/helicase: an ATP switch regulates the cooperativity among the different substrate binding sites. *Biochemistry* 41, 10332-10342
- 52. Luik, P., Chew, C., Aittoniemi, J., Chang, J., Wentworth, P., Jr., Dwek, R. A., Biggin, P. C., Venien-Bryan, C., and Zitzmann, N. (2009) The 3-dimensional structure of a hepatitis C virus p7 ion channel by electron microscopy. *Proceedings of the National Academy of Sciences of the United States of America* 106, 12712-12716
- 53. Welker, M. W., Welsch, C., Meyer, A., Antes, I., Albrecht, M., Forestier, N., Kronenberger, B., Lengauer, T., Piiper, A., Zeuzem, S., and Sarrazin, C. (2010) Dimerization of the hepatitis C virus nonstructural protein 4B depends on the integrity of an aminoterminal basic leucine zipper. *Protein science: a publication of the Protein Society* 19, 1327-1336
- 54. Merola, M., Brazzoli, M., Cocchiarella, F., Heile, J. M., Helenius, A., Weiner, A. J., Houghton, M., and Abrignani, S. (2001) Folding of hepatitis C virus E1 glycoprotein in a cell-free system. *Journal of virology* 75, 11205-11217
- 55. Lo, S. Y., Selby, M. J., and Ou, J. H. (1996) Interaction between hepatitis C virus core protein and E1 envelope protein. *Journal of virology* 70, 5177-5182
- 56. Grakoui, A., Wychowski, C., Lin, C., Feinstone, S. M., and Rice, C. M. (1993) Expression and identification of hepatitis C virus polyprotein cleavage products. *Journal of virology* 67, 1385-1395
- 57. Lanford, R. E., Notvall, L., Chavez, D., White, R., Frenzel, G., Simonsen, C., and Kim, J. (1993) Analysis of hepatitis C virus capsid, E1, and E2/NS1 proteins expressed in insect cells. *Virology* 197, 225-235
- 58. Whidby, J., Mateu, G., Scarborough, H., Demeler, B., Grakoui, A., and Marcotrigiano, J. (2009) Blocking hepatitis C virus infection with recombinant form of envelope protein 2 ectodomain. *Journal of virology* 83, 11078-11089
- 59. Clarke, D., Griffin, S., Beales, L., Gelais, C. S., Burgess, S., Harris, M., and Rowlands, D. (2006) Evidence for the formation of a heptameric ion channel complex by the hepatitis C virus p7 protein in vitro. *The Journal of biological chemistry* 281, 37057-37068
- 60. Stapleford, K. A., and Lindenbach, B. D. (2011) Hepatitis C virus NS2 coordinates virus particle assembly through physical interactions with the E1-E2 glycoprotein and NS3-NS4A enzyme complexes. *Journal of virology* 85, 1706-1717
- 61. Tedbury, P., Welbourn, S., Pause, A., King, B., Griffin, S., and Harris, M. (2011) The subcellular localization of the hepatitis C virus non-structural protein NS2 is regulated by an ion channel-independent function of the p7 protein. *The Journal of general virology* 92, 819-830
- 62. Lorenz, I. C., Marcotrigiano, J., Dentzer, T. G., and Rice, C. M. (2006) Structure of the catalytic domain of the hepatitis C virus NS2-3 protease. *Nature* 442, 831-835
- 63. Jones, D. M., Atoom, A. M., Zhang, X., Kottilil, S., and Russell, R. S. (2011) A genetic interaction between the core and NS3 proteins of hepatitis C virus is essential for production of infectious virus. *Journal of virology* 85, 12351-12361
- 64. Schregel, V., Jacobi, S., Penin, F., and Tautz, N. (2009) Hepatitis C virus NS2 is a protease stimulated by cofactor domains in NS3. *Proceedings of the National Academy of Sciences of the United States of America* 106, 5342-5347
- 65. Gallinari, P., Brennan, D., Nardi, C., Brunetti, M., Tomei, L., Steinkuhler, C., and De Francesco, R. (1998) Multiple enzymatic activities associated with recombinant NS3 protein of hepatitis C virus. *Journal of virology* 72, 6758-6769

- 66. Bartenschlager, R., Lohmann, V., Wilkinson, T., and Koch, J. O. (1995) Complex formation between the NS3 serine-type proteinase of the hepatitis C virus and NS4A and its importance for polyprotein maturation. *Journal of virology* 69, 7519-7528
- 67. Failla, C., Tomei, L., and De Francesco, R. (1994) Both NS3 and NS4A are required for proteolytic processing of hepatitis C virus nonstructural proteins. *Journal of virology* 68, 3753-3760
- 68. Lin, C., Pragai, B. M., Grakoui, A., Xu, J., and Rice, C. M. (1994) Hepatitis C virus NS3 serine proteinase: trans-cleavage requirements and processing kinetics. *Journal of virology* 68, 8147-8157
- 69. Tanji, Y., Hijikata, M., Satoh, S., Kaneko, T., and Shimotohno, K. (1995) Hepatitis C virus-encoded nonstructural protein NS4A has versatile functions in viral protein processing. *Journal of virology* 69, 1575-1581
- 70. Paredes, A. M., and Blight, K. J. (2008) A genetic interaction between hepatitis C virus NS4B and NS3 is important for RNA replication. *Journal of virology* 82, 10671-10683
- 71. Lin, C., Wu, J. W., Hsiao, K., and Su, M. S. (1997) The hepatitis C virus NS4A protein: interactions with the NS4B and NS5A proteins. *Journal of virology* 71, 6465-6471
- 72. Yu, G. Y., Lee, K. J., Gao, L., and Lai, M. M. (2006) Palmitoylation and polymerization of hepatitis C virus NS4B protein. *Journal of virology* 80, 6013-6023
- 73. Masaki, T., Suzuki, R., Murakami, K., Aizaki, H., Ishii, K., Murayama, A., Date, T., Matsuura, Y., Miyamura, T., Wakita, T., and Suzuki, T. (2008) Interaction of hepatitis C virus nonstructural protein 5A with core protein is critical for the production of infectious virus particles. *Journal of virology* 82, 7964-7976
- 74. Miyanari, Y., Atsuzawa, K., Usuda, N., Watashi, K., Hishiki, T., Zayas, M., Bartenschlager, R., Wakita, T., Hijikata, M., and Shimotohno, K. (2007) The lipid droplet is an important organelle for hepatitis C virus production. *Nature cell biology* 9, 1089-1097
- 75. Goh, P. Y., Tan, Y. J., Lim, S. P., Lim, S. G., Tan, Y. H., and Hong, W. J. (2001) The hepatitis C virus core protein interacts with NS5A and activates its caspase-mediated proteolytic cleavage. *Virology* 290, 224-236
- 76. Lundin, M., Lindstrom, H., Gronwall, C., and Persson, M. A. (2006) Dual topology of the processed hepatitis C virus protein NS4B is influenced by the NS5A protein. *The Journal of general virology* 87, 3263-3272
- 77. Love, R. A., Brodsky, O., Hickey, M. J., Wells, P. A., and Cronin, C. N. (2009) Crystal structure of a novel dimeric form of NS5A domain I protein from hepatitis C virus. *Journal of virology* 83, 4395-4403
- 78. Tellinghuisen, T. L., Marcotrigiano, J., and Rice, C. M. (2005) Structure of the zinc-binding domain of an essential component of the hepatitis C virus replicase. *Nature* 435, 374-379
- 79. Uchida, M., Hino, N., Yamanaka, T., Fukushima, H., Imanishi, T., Uchiyama, Y., Kodama, T., and Doi, T. (2002) Hepatitis C virus core protein binds to a C-terminal region of NS5B RNA polymerase. *Hepatology research: the official journal of the Japan Society of Hepatology* 22, 297-306
- 80. Kang, S. M., Choi, J. K., Kim, S. J., Kim, J. H., Ahn, D. G., and Oh, J. W. (2009) Regulation of hepatitis C virus replication by the core protein through its interaction with viral RNA polymerase. *Biochemical and biophysical research communications* 386, 55-59
- 81. Zhang, C., Cai, Z., Kim, Y. C., Kumar, R., Yuan, F., Shi, P. Y., Kao, C., and Luo, G. (2005) Stimulation of hepatitis C virus (HCV) nonstructural protein 3 (NS3) helicase activity by the NS3 protease domain and by HCV RNA-dependent RNA polymerase. *Journal of virology* 79, 8687-8697
- 82. Ishido, S., Fujita, T., and Hotta, H. (1998) Complex formation of NS5B with NS3 and NS4A proteins of hepatitis C virus. *Biochemical and biophysical research communications* 244, 35-40

- 83. Shirota, Y., Luo, H., Qin, W., Kaneko, S., Yamashita, T., Kobayashi, K., and Murakami, S. (2002) Hepatitis C virus (HCV) NS5A binds RNA-dependent RNA polymerase (RdRP) NS5B and modulates RNA-dependent RNA polymerase activity. *The Journal of biological chemistry* 277, 11149-11155
- 84. Costes, S. V., Daelemans, D., Cho, E. H., Dobbin, Z., Pavlakis, G., and Lockett, S. (2004) Automatic and quantitative measurement of protein-protein colocalization in live cells. *Biophysical journal* 86, 3993-4003
- 85. Saito, R., Smoot, M. E., Ono, K., Ruscheinski, J., Wang, P. L., Lotia, S., Pico, A. R., Bader, G. D., and Ideker, T. (2012) A travel guide to Cytoscape plugins. *Nature methods* 9, 1069-1076

Figure legends

Figure 1: Characterization of HCV-CFP and -YFP fusion proteins. All fusion proteins used in this study and characterized here carry an N-terminal chromophore tag. (A) 300.000 293T cells were transfected with 5 μg DNA of each HCV CFP/YFP fusion protein in a 6-well format. Cellular lysates were generated for WB and expression of the fusion proteins was detected by an antibody specific for various chromophores including CFP and YFP. Actin was blotted as loading control. (B) 150.000 293T cells were transfected with 2.5 μg DNA in a 12-well format. The mean fluorescence intensity and the percentage of cells transfected with the HCV-YFP fusion proteins were assessed by FACS analysis. Mean values and standard deviations are calculated from at least four independent transfections. (C) Transfections and measurements were done similar to (B) but with the HCV-CFP fusions. Then the mean values for fluorescence intensity and percentage transfected cells were correlated. Squared Pearson's correlation (R²) and corresponding p-values were calculated with Graph Pad Prism 5.0. (D) 293T cells transfected with the

indicated HCV-YFP fusion proteins and GalT-CFP were grown on cover slips and embedded for confocal microscopy. The scale bar indicates a distance of 7 µm.

Figure 2: FRET analysis of specific HCV protein interactions. 293T and Huh7.5 cells were transfected with (A) CFP-E2 and YFP-E1, (B) CFP-Core and YFP-Core or (C) CFP-E2 and YFP-NS3. Panel 1 shows the subcellular distribution of the respective YFP (green) and CFP (red) fusions, as well as areas of colocalization (yellow) in 293T cells. The scale bar gives a length of 7 μm. Panel 2 depicts examples of primary FACS plots acquired for FRET analysis. Panel 3 shows the mean value of the percentage of cells scoring FRET+ (MF) and the according standard deviation across multiple independent transfections (n=3-17).

Figure 3: Overview of HCV protein interactions measured via FACS-FRET in both tested cell lines. Statistical significant interactions with FRET values ≥10 % are presented (compare Supplemental Figure S1). Interactions in 293T are highlighted by dark green boxes and those which were also significant in Huh7.5 are coloured in fading green. Furthermore we marked interactions which were previously described by others (black underscored bar, numbers of the corresponding references are written in the boxes). Interactions which are newly reported by this study are highlighted by a check mark. Figure References: (5, 8, 13-16, 24-28, 50-83).

The inlay depicts the correlation of FACS-FRET results generated in 293T and Huh7.5 liver cells. Mean values of the % FRET+ cells derived from 293T transfection

were plotted with the according values obtained from Huh7.5 transfections (n=45, compare Figure S1). Pearson's correlation and the corresponding p-value were calculated with Graph Pad Prism 5.0.

Figure 4: Novel HCV protein interactions detected by FACS-FRET. Panel 1 gives mean values of % FRET+ cells and standard deviations of multiple independent experiments (for number of replicates (n), mean FRET values (MF) and standard deviations (SD) as well as statistical calculations please refer to Supplemental Figure S1). We further present representative confocal images of 293T and Huh7.5 cells which were transfected with the indicated CFP (red) and YFP (green) fusion proteins in panel 2. Colocalization in the overlay appears yellow. The scale bar is 7 μm. (A) CFP-E2 and YFP-p7, CFP-NS5B and YFP-E1 as well as CFP-NS5B and YFP-E2 showed significant FRET in both cell lines whereas (B) CFP-E2 and YFP-Core, CFP-NS2 and YFP-Core, CFP-p7 and YFP-Core as well as CFP-p7 and YFP-E1 only exerted FRET in 293T cells.

Figure 5: JFH1 p7-RR33/35QQ differentially interacts with Core, E1 and E2. (A) Primary FACS-FRET plots of 293T cells transfected with the indicated CFP and YFP fusion proteins. Please note that for p7 self-interaction we cotransfected either the p7-CFP and p7-YFP plasmid or the p7-RR/QQ-CFP together with the p7-RR/QQ-YFP. (B) Mean values of % FRET+ cells and standard deviations of seven independent transfections performed as indicated in (A). For calculation of statistical

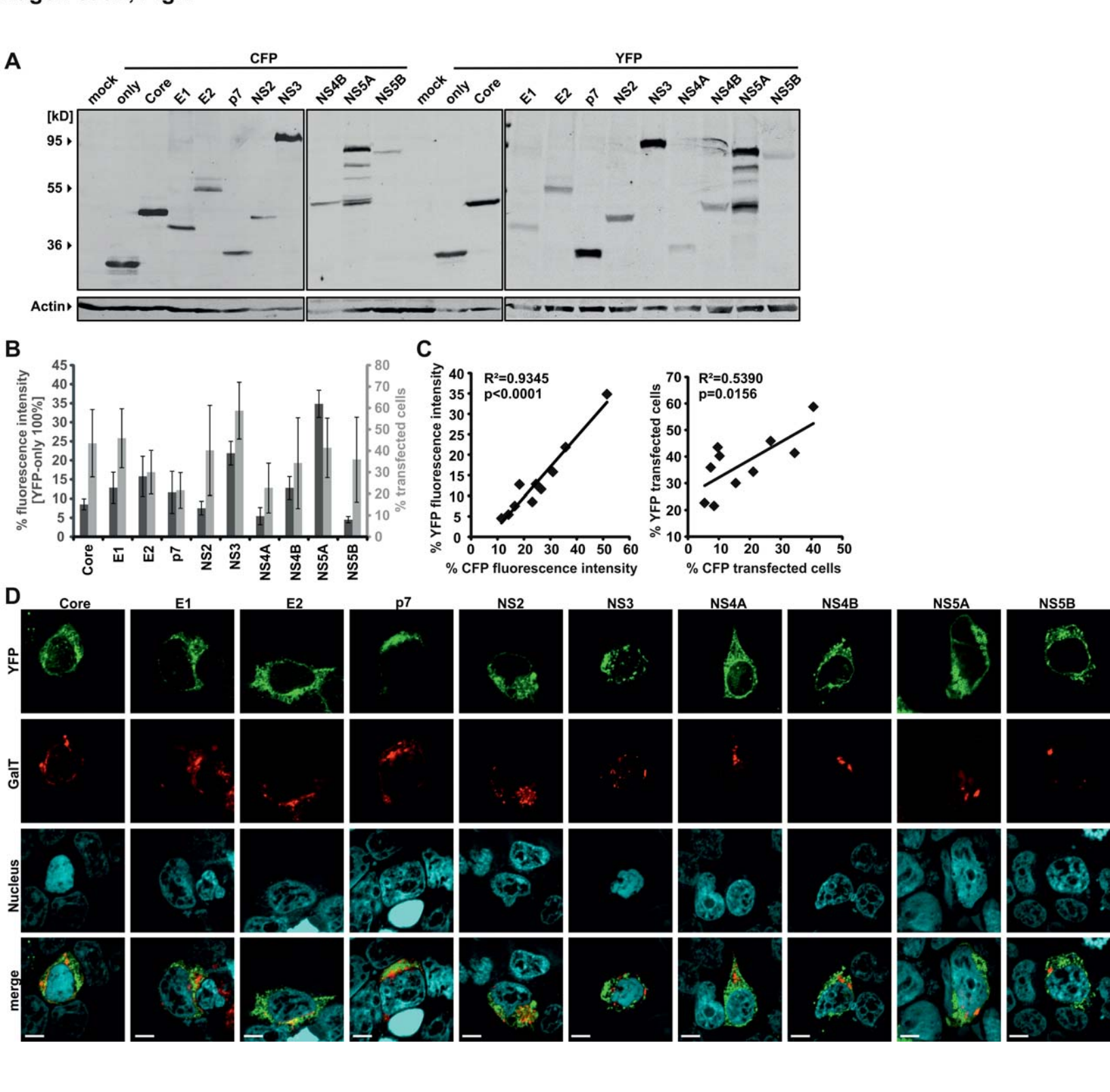
significance, mean FRET signals were compared with the two-tailed unpaired Student's t test (Graph Pad Prism 5.0).

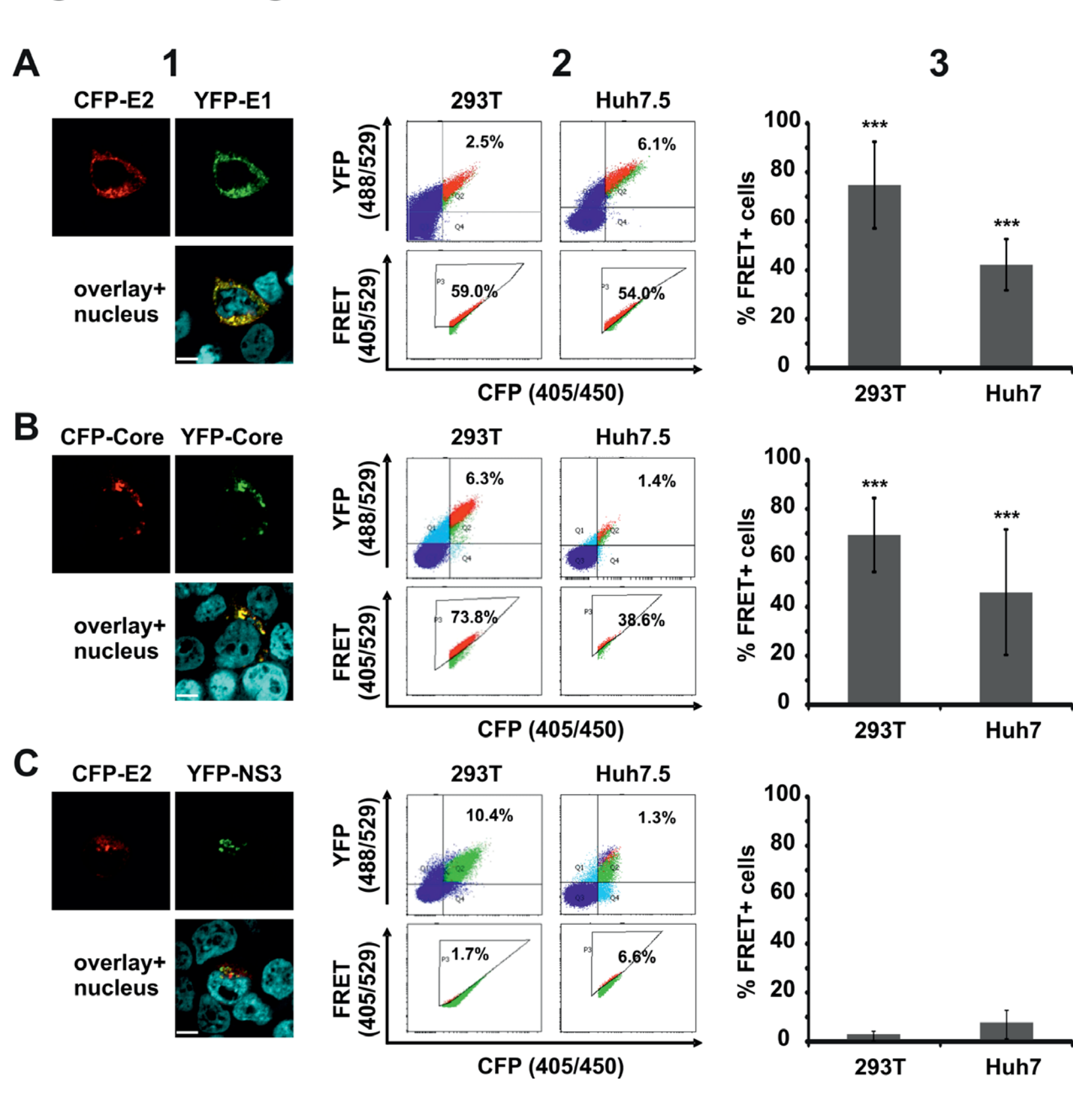
Figure 6: Viral structural proteins coimmunoprecipitate with p7 in lysates of HCV expressing Huh7.5 cells. Huh7.5 cells were RNA electroporated with either (1) no RNA, (2) HCV Jc1-E1(A4) or (3) HCV Jc1-E1(A4)-p7(HA) allowing to detect E1 by the A4 antibody (8) and p7 with an anti-HA antibody. Then p7(HA) was immunoprecipitated with a rabbit derived anti-HA antibody (upper bands) or a mouse derived anti-HA antibody (lower bands). Core, E1, E2 and p7 were detected in lysates and post precipitation by immunoblot.

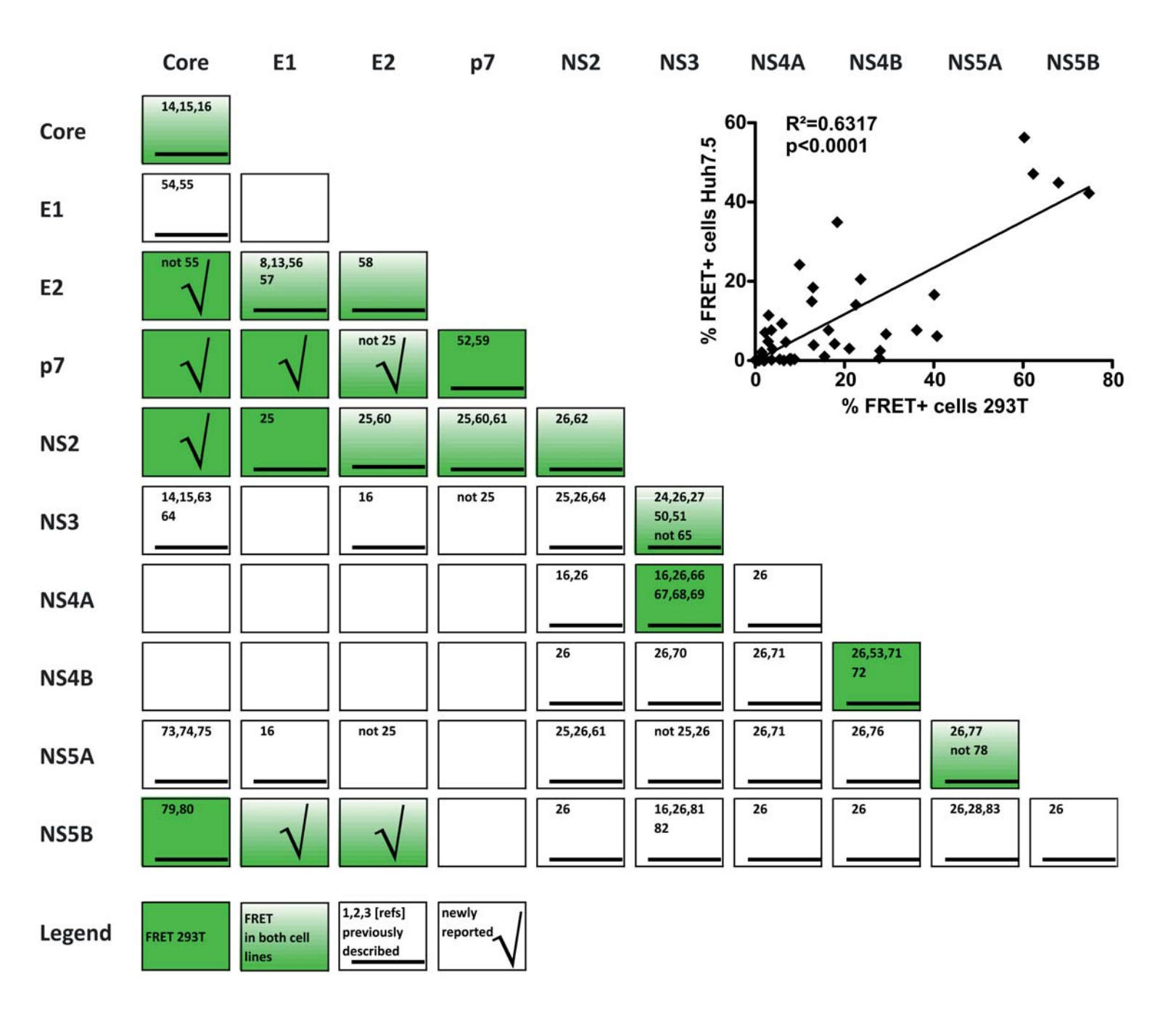
Figure 7: Viral structural proteins colocalize with p7 in HCV expressing Huh7.5 cells. Huh7.5 cells were RNA electroporated with the indicated HCV constructs. Then immunofluorescence staining with specific antibodies was performed to detect areas of protein colocalization by confocal microscopy. We quantified colocalization by Costes Pearson's correlation (84). (A) Depicts examples of confocal images. The squared Pearson's correlation coefficient (R²) is indicated in the merged image. The scale bar has a length of 5 μm. (B) Each dot represents the R² correlation for one analysed cell. Mean values of at least twelve measured cells per colocalization analyses were plotted and assessed for significant differences with one way ANOVA test (Graph Pad Prism 5.0): p<0.01 (*), p<0.001 (**) and p<0.0001 (***).

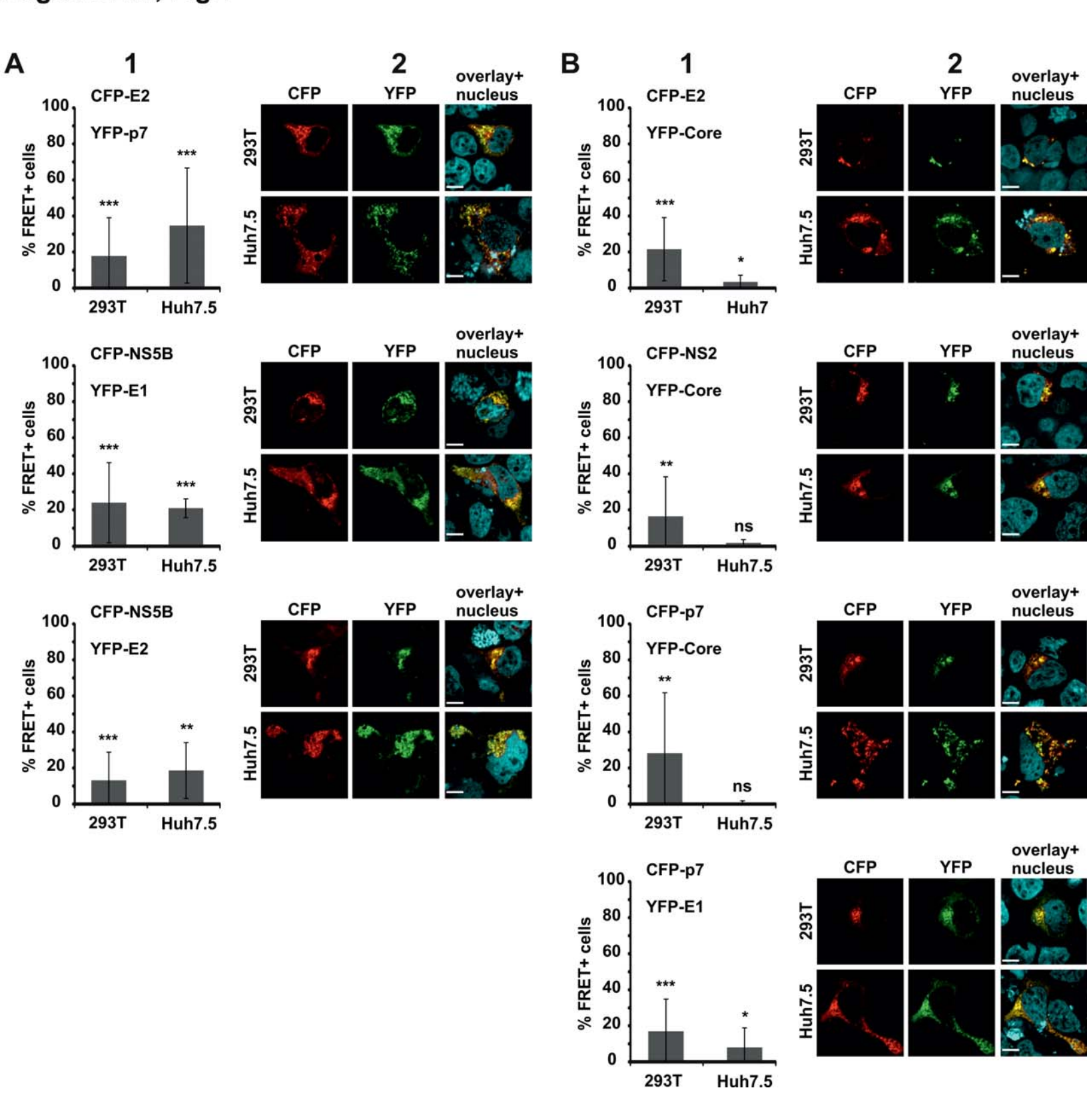
Figure 8: Viral structural proteins interact with p7 in HCV expressing intact Huh7.5 cells. Huh7.5 cells were RNA electroporated with the indicated HCV constructs. Then staining for proximity ligation assay (PLA) was done with the same antibodies that were used for colocalization analyses (compare Fig. 7). We quantified positive PLA events by software based counting of red dots and normalized this to the number of cells (nuclear DAPI staining). (A) Representative examples of PLA images are shown. Indicated are the antibodies, which were used for the primary PLA stain and the amount of PLA dots, identified by software counting. The scale bar has a length of 5 μm. (B) Each dot represents the number of PLA spots counted for one cell per image. Mean values of at least eight measurements per antibody pair were plotted and assessed for significant differences with one way ANOVA test (Graph Pad Prism 5.0): p<0.01 (*), p<0.001 (**) and p<0.0001 (***).

Figure 9: The HCV protein interaction network. HCV protein interactions measured in this study by FRET (red lines) or reported previously (dotted grey lines) were visualized as a network. Furthermore, HCV protein interactions with host cell factors were incorporated by using interaction data from the VirusMINT database and de Chassey et al. (4). This network was generated with Cytoscape ((85), www.cytoscape.org).









Hagen et al., Fig.5

